Phase diagram of a modulated relaxation oscillator with a finite resetting time

Bo Christiansen
Physics Laboratory, University of Copenhagen, H. C. Ørsted Institute, Universitetsparken 5, DK-2100 Copenhagen Ø, Denmark

Da-Ren He,* S. Habip, M. Bauer, U. Krueger, and W. Martienssen
Physikalisches Institut der Universität, D-6000 Frankfurt am Main 11, Germany
(Received 14 February 1992)

A modulated relaxation oscillator with a finite resetting time is considered. The underlying return map, a combination of a circle map and an inverse circle map, is deduced. Two critical lines, associated with an inflection point and a point of infinite slope in the return map, respectively, divide the parameter space into four regions of qualitatively different behavior. One region is chaotic, as the return map is not invertible. In another region, a gap exists in the return map and only periodic attractors are possible. In a third region, the return map simultaneously is noninvertible and contains a gap, which gives rise to a wide range of nonlinear phenomena. The critical lines are found analytically and the structure of the phase-locked steps is studied.

PACS number(s): 05.45.+b, 84.30.−r

I. INTRODUCTION

Relaxation oscillators and "integrate-and-fire" models have been a topic of many recent studies. A system may be described by an integrate-and-fire model if trajectories are weakly attracted to a strongly repellent region in phase space. The trajectories are then pushed away from this region much faster than they are attracted to it. Thus a hallmark for these systems is the existence of two different time scales. A wide range of physical, chemical, and biological systems is well described by these models. Examples are charge-density-wave systems [1], the Belousov-Zhabotinskii reaction [2,3] neuronal encoding [4–6] the dripping faucet [7], and geysers. Furthermore, many electronic oscillators (e.g., the neon lamp) fall into this category [8]. Apart from the practical importance, these systems are of theoretical interest due to the wide range of nonlinear phenomena they exhibit. In particular, they show two types of supercritical behavior. In some parts of phase space the phase-locked steps overlap and chaos is encountered. In addition to this behavior, characteristic for circle-map-like systems, other parts of phase space are found where the phase locking stays complete and only periodic attractors exist. These regions and the transitions between them have previously been studied [9–13].

These studies, however, have been done in the limit of abrupt resetting, i.e., the short time scale has been modeled by a discontinuity. Considering that most practical relaxation oscillators are only crudely described by this simplification, we are presenting a study of a more realistic model, composed of exponential growth and decay between a sine-modulated upper threshold and a constant lower threshold. In this paper we report analytical and numerical results on critical lines, phase-locked steps and Lyapunov exponents.

The paper is organized as follows. In Sec. II the system is described and the return map is deduced. Section III regards the critical lines, while in Sec. IV we treat the Lyapunov exponents. In Sec. V the structure of the phase-locked regions is considered and numerical results are presented. We close the paper in Sec. VI, with a discussion of its relation to previous work.

II. THE SYSTEM

The system we want to consider is drawn from a practical thyratron relaxation oscillator, the physics of which has been reported in detail elsewhere [14,15]. For our present analytical studies the system can be suitably described by the following one-dimensional integrate-and-fire model. The "voltage" $V(t)$, the only variable, increases according to

$$\dot{V}=I-V/\tau_u \ , \tag{1}$$

until an upper threshold $T(t)$ is reached at τ_1, i.e., $V(\tau_1)=T(\tau_1)$. At this instant the time evolution of V is abruptly changed to

$$\dot{V}=I-V/\tau_d \ . \tag{2}$$

For a suitable choice of parameters, V then decreases until a lower threshold $B(t)$ is reached at time t_1, i.e., $V(t_1)=B(t_1)$. Again V increases, satisfying Eq. (1) until the upper threshold is reached once more at time τ_2, etc. At times t_i and τ_i, $i=1,2,\ldots$, the system is said to fire. Both Eqs. (1) and (2) include damping in addition to the linear term I and the constants τ_u and τ_d determine the two different time scales. We note that while V is continuous, $\dot{V}$ is discontinuous as the damping constant changes at the firing times. It is this discontinuity that gives rise to the nonlinear phenomena, otherwise found only in (continuous) systems of higher order. In the present case the upper threshold is modulated $T(t)=A_0-A\sin(\omega t)$, while the lower threshold is kept

constant $B(t)=B_0$. Figure 1 shows the time evolution of the system.

A scaling of the system, including a time scaling, allows us without loss of generality to write the system in normalized form with $B_0=1$ and $\omega=2\pi$. We are then left with the five independent parameters A_0, A, I, τ_u, τ_d.

When the fixed point $V=I\tau_u$ of Eq. (1) is less than the minimum A_0-A of the upper threshold $T(t)$, the system relaxes to this fixed point. This means that the region $I\tau_u < A_0-A$ in parameter space is nonfiring. The same conclusion can be obtained for the region $I\tau_d > B_0$.

We now define the maps f, g, and h by $\tau_n=f(t_{n-1})$, $t_n=g(\tau_n)$, and $t_{n+1}=h(t_n)=g\circ f(t_n)$. From Eqs. (1) and (2) we have

$$f(t)=t-\tau_u \ln\frac{I\tau_u-T(f(t))}{I\tau_u-B_0} \tag{3}$$

and

$$g(t)=t-\tau_d \ln\frac{I\tau_d-B_0}{I\tau_d-T(t)} \ . \tag{4}$$

The function $f(t)$ is only implicitly given by Eq. (3). In a supercritical region $f(t)$ is multivalued. The geometry of the system (see Fig. 1) then tells us to choose the lowest value for f. A map of this kind is called an "inverse circle map" [14,10,11]. It shows the same dynamics as the circle map in the subcritical region of parameter space, while it is completely phase locked in the supercritical region. The map $g(t)$ is an ordinary circle map. The function $h(t)$, which is the underlying return map of the system under consideration, is then a combination of an ordinary and an inverse circle map.

A useful parameter to characterize the attractors is the firing number R, i.e., the average number of firings in one period of the modulation

$$R=\lim_{n\to\infty}\frac{2\pi}{\omega}\frac{n}{h^n(t_0)} \ . \tag{5}$$

For periodic attractors the firing number is rational. The firing number is simply the reciprocal of the more commonly used rotation number.

III. THE CRITICAL LINES

We denote the critical lines, where either a point with infinite slope or an inflection point appears in the return map $h(t)$, by l_1 and l_2, respectively. They are both determined by the criterion

$$V(t)=T(t) \ , \quad \dot{V}(t)=\dot{T}(t) \ , \quad \ddot{V}(t)=\ddot{T}(t) \ , \tag{6}$$

where the dot indicates differentiation with respect to time. Each critical line divides the parameter space in a subcritical and a supercritical region. In the subcritical region the increasing voltage is always steeper than the threshold at times of firing. However, in the supercritical region with respect to l_1, a time t_c exists, when the increasing branch of the voltage tangentially meets the upper threshold. In the supercritical region the result is the shadowing of parts of the threshold and the existence of a corresponding gap in the return map. The gap emerges as a point of vertical slope on the critical line l_1, where $V(t)$ and $T(t)$ near t_c are identical to third order. The mechanism responsible for the gap is that of a cusp catastrophe [16]. A similar geometrical interpretation can be given for the other critical line l_2. From Eqs. (1), (2), and (6) we get, after some algebra,

$$\begin{aligned} I\tau_u &= A_0+A[1+(\tau_u\omega)^2]^{1/2} \quad (l_1) \\ I\tau_d &= A_0-A[1+(\tau_d\omega)^2]^{1/2} \quad (l_2) \ . \end{aligned} \tag{7}$$

In the (A,I) space the critical curves are straight lines. The lines intersect in (A_c, I_c) and divide the parameter space into four regions. Figure 2 shows the critical lines in (A,I) space for $A_0=1.5$, $\tau_u=5$, and $\tau_d=0.5$ and names the regions I, II, III, and IV.

Figure 3(a) shows the return map $s_{i+1}=h(s_i)\mathrm{mod}(2\pi/\omega)$ for a set of parameters in region I. In this region the return map is one to one and the attrac-

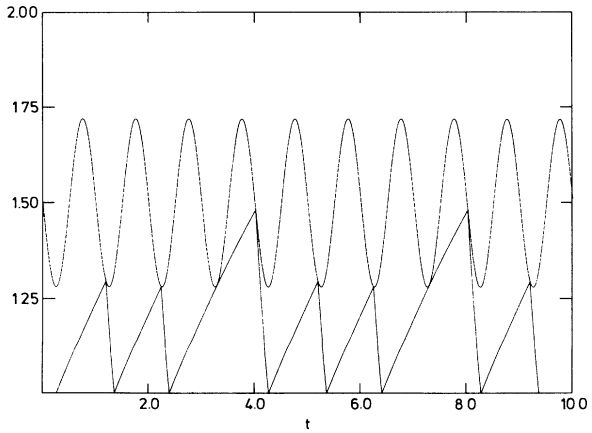

FIG. 1. Time evolution of the relaxation oscillation described by Eq. (1) and (2). The upper curve is $T(t)$ and the lower curve is $V(t)$. The parameters are $I=0.55$, $A=0.22$, $\tau_u=5$, $\tau_d=0.5$, $A_0=1.5$, $B_0=1$, and $\omega=2\pi$.

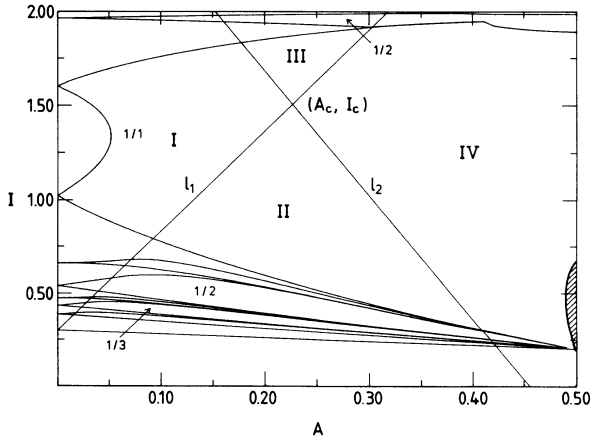

FIG. 2. The critical lines l_1 and l_2 and the different regions in (A,I) space. The parameters are $\tau_u=5$, $\tau_d=0.5$, $A_0=1.5$, $B_0=1$, and $\omega=2\pi$.

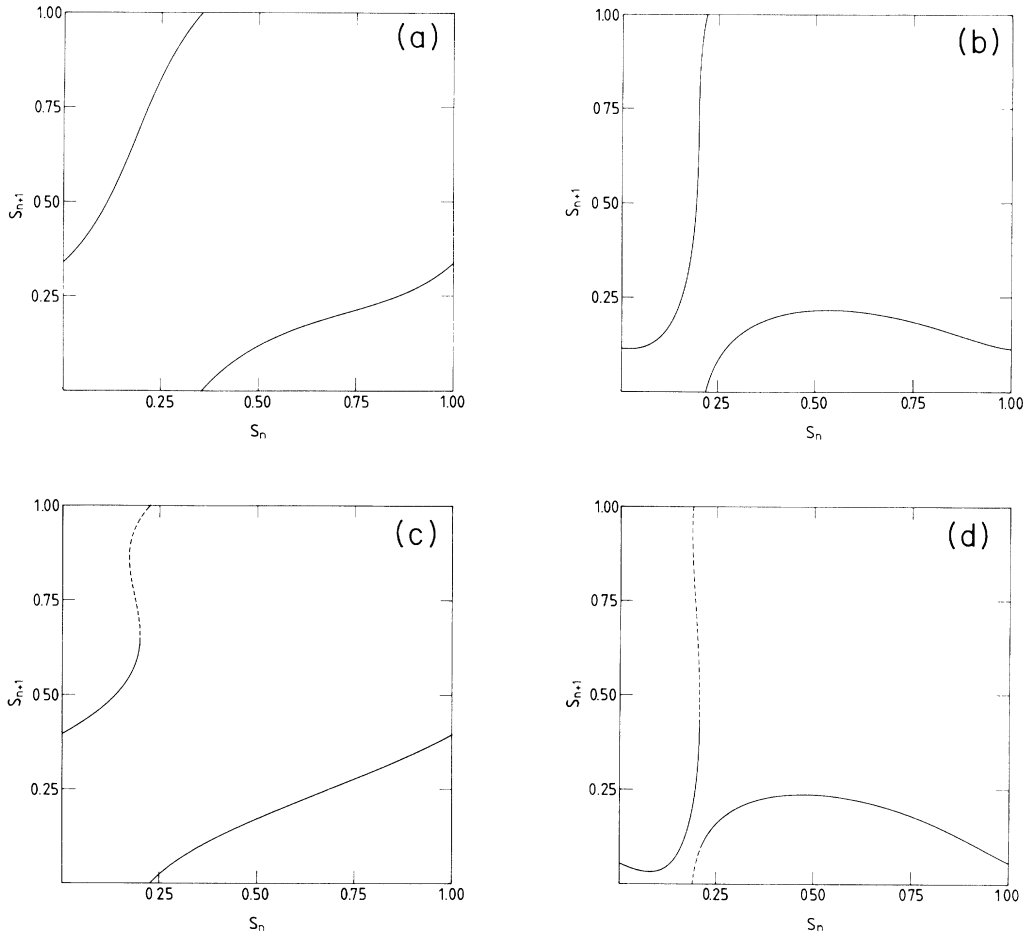

FIG. 3. Return maps in the different regions of parameter space: (a) in region I with $A=0.1$ and $I=1.9$; (b) in region III with $A=0.033$ and $I=0.47$; (c) in region II with $A=0.25$ and $I=1.9$; and (d) in region IV with $A=0.3$ and $I=1.9$. The other parameters are $\tau_u=5$, $\tau_d=0.5$, $A_0=1.5$, $B_0=1$, and $\omega=2\pi$. In (c) and (d) the gap is indicated by a dashed line.

tors are either periodic or quasiperiodic. By increasing the amplitude A and thereby the nonlinearity, two different transitions are possible. If I is less than I_c the critical line l_1 will be crossed and a gap will appear in the return map as we enter region II [Fig 3(c)]. In this region the return map is invertible but discontinuous and we have complete phase locking (CPL). If on the other hand I is greater than I_c the line l_2 will be crossed and a noninvertibility appears in the return map as we enter region III. In this region the return map is continuous but noninvertible [Fig. 3(b)] and the phase-locked steps, complete on l_2, will start to overlap, creating chaos in the way well known from circle-map studies.

Increasing A further, region IV is reached either via l_1, generating a gap in the noninvertible map, or via l_2, generating a noninvertibility in the discontinuous map. In region IV the return map is then both noninvertible and contains a gap [Fig. 3(d)], having the potential for both CPL and chaos. We will show elsewhere how the type of attractors in this region depends on the exact choice of parameters. In Sec. V we give a more detailed discussion of the structure of the phase-locked steps in the four regions of parameter space.

IV. THE LYAPUNOV EXPONENT

One of the major tools in the theoretical and experimental study of non-Hamiltonian dynamic systems is the spectrum of Lyapunov exponents. It allows one to discriminate between periodic, quasiperiodic, and chaotic attractors and gives an estimate of the fractal dimension of the attractor. Each exponent expresses the average divergence of nearby trajectories along a principal axis and the sum of the exponents equals the average damping on the attractor. In the simple one-dimensional case, only three qualitatively different possibilities exist: the single Lyapunov exponent is negative, zero, or positive, corresponding to a periodic, quasiperiodic, or chaotic attractor, respectively. As the average damping is positive in the chaotic case, the term attractor is not used here in the usual meaning of an attracting region of zero volume in phase space. The one-dimensional phase space does not support the distinction between volume and length.

In the present case the Lyapunov number L is determined by

$$L=\lim_{n\to\infty}\prod_{i=1}^{n}L_i^{1/n}\ , \tag{8}$$

where L_i is the Lyapunov number in the interval $[t_i-1,t_i]$. The number L_i can be written as a product of four factors $L_i=L_i^1L_i^2L_i^3L_i^4$, where L_i^1 and L_i^2 originate from the increasing and decreasing parts of V, respectively. These contributions to the Lyapunov exponent $\lambda=\ln|L|$ [17] are always negative, owing to the damping terms. From Eqs. (1) and (2) we get

$$L_i^1=\exp[-(\tau_i-t_i-1)/\tau_u]=\frac{I\tau_u-T(\tau_i)}{I\tau_u-B_0} \tag{9}$$

and

$$L_i^2=\exp[-(t_i-\tau_i)/\tau_d]=\frac{I\tau_d-B_0}{I\tau_d-T(\tau_i)} . \tag{10}$$

The remaining terms L_i^3 and L_i^4 arise from the discontinuous firing processes. To find L_i^3 we consider a firing on the upper threshold at time τ_i. Let δV_b and δV_a be the infinitesimal differences between two trajectories immediately before and immediately after the firing (see Fig. 4). The two trajectories fire with an infinitesimal disparity δt in time. We now linearize V and T about τ_i. Then the slope of V is $S_b=I-T(\tau_i)/\tau_u$ before the firing, $S_a=I-T(\tau_i)/\tau_d$ after the firing, and the slope of T is simply $\dot{T}(\tau_i)$. From Fig. 4 we find

$$\delta V_b+\dot{T}(\tau_i)\delta t=S_b\delta t \tag{11}$$

and

$$\delta V_a+\dot{T}(\tau_i)\delta t=S_a\delta t . \tag{12}$$

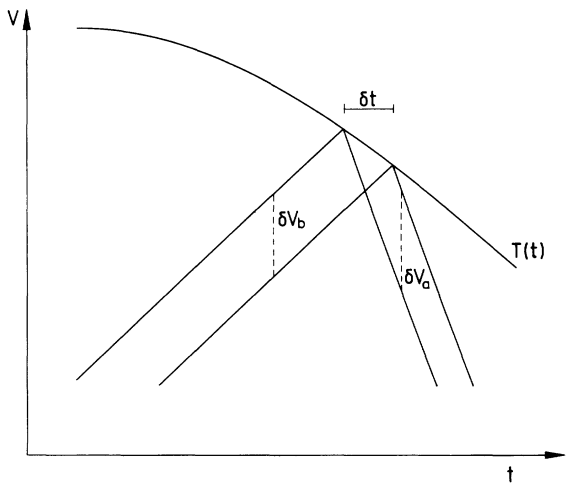

FIG. 4. Trajectories initially separated by a distance δV_b will, after a firing, be separated by δV_a. The difference in firing time is δt.

We now have

$$L_i^3=\frac{\delta V_a}{\delta V_b}=\frac{S_a-\dot{T}(\tau_i)}{S_b-\dot{T}(\tau_i)} . \tag{13}$$

Analogously we find, by considering a firing on the lower threshold,

$$L_i^4=\frac{I-B_0/\tau_u}{I-B_0/\tau_d} . \tag{14}$$

Equation (8) now reads

$$L=\lim_{n\to\infty}\prod_{i=1}^{n}\frac{1-\dot{T}(\tau_i)/S_a}{1-\dot{T}(\tau_i)/S_b}=\lim_{n\to\infty}\prod_{i=1}^{n}\left[\frac{[I\tau_u-T(\tau_i)][I\tau_d-T(\tau_i)-\tau_d\dot{T}(\tau_i)]}{[I\tau_d-T(\tau_i)][I\tau_u-T(\tau_i)-\tau_u\dot{T}(\tau_i)]}\right]^{1/n} . \tag{15}$$

The positive contributions to the Lyapunov number come from both types of firings. But while L_i^4 is a constant, L_i^3 depends on the time of the firing. In particular, this contribution will be important if the increasing voltage and the threshold T are close to parallel when the system fires. In the next section we present figures based on formula (15).

V. THE PHASE-LOCKED STEPS

In this section we consider the phase-locked steps in parameter space. In particular, we will study their positions and shapes in the (A,I) subspace, keeping τ_u, τ_d, A_0, B_0, and ω fixed. To this end we first consider the fully solvable case when the modulation is absent, $A=0$. We first note from Eq. (15) that $|L|=1$, so all attractors are quasiperiodic. From Eqs. (3) and (4) $h(t)$ is found to be linear with the unit slope and the firing number is then easily determined by its definition [Eq. (5)]

$$R=\frac{2\pi}{\omega}\left[\ln\left[\frac{I\tau_u-B_0}{I\tau_u-A_0}\right]^{\tau_u}\left[\frac{A_0-I\tau_d}{B_0-I\tau_d}\right]^{\tau_d}\right]^{-1} . \tag{16}$$

We note that the firing number becomes zero when I reaches the edges A_0/τ_u and B_0/τ_d of the nonfiring regions, as should be expected. Close to the edges of the nonfiring regions, Eq. (16) takes the form $R=-(2\pi/\omega)[\tau_u\ln(I-A_0/\tau_u)]^{-1}$ and $R=-(2\pi/\omega)[\tau_d\ln(B_0/\tau_d-I)]^{-1}$, respectively. This gives a vertical slope dR/dI at the edges. Figure 5 shows R as a function of I. The firing number has a maximum $R_{\max}$ for $I=I_{\max}$, and is asymmetrical with its steepest part for $I>I_{\max}$ (as $\tau_u>\tau_d$).

When modulated, the system develops phase-locked steps. The criterion for an attractor to be phase locked on the P/Q step is

$$h^P(t_0)=t_0+\frac{2\pi}{\omega}Q . \tag{17}$$

This equation expresses the periodicity of the attractor.

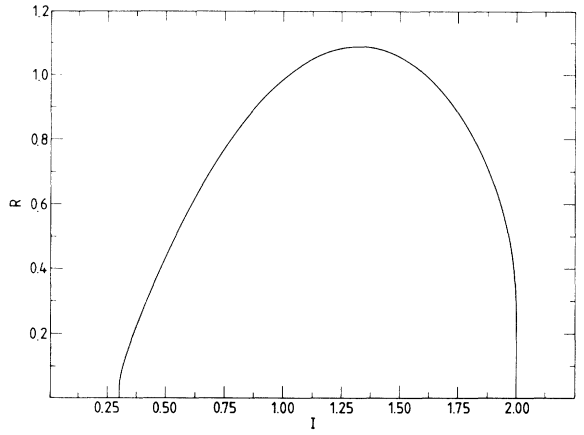

FIG. 5. The firing number R as a function of I when modulation is absent, $A=0$. The other parameters are $\tau_u=5$, $\tau_d=0.5$, $A_0=1.5$, $B_0=1$, and $\omega=2\pi$.

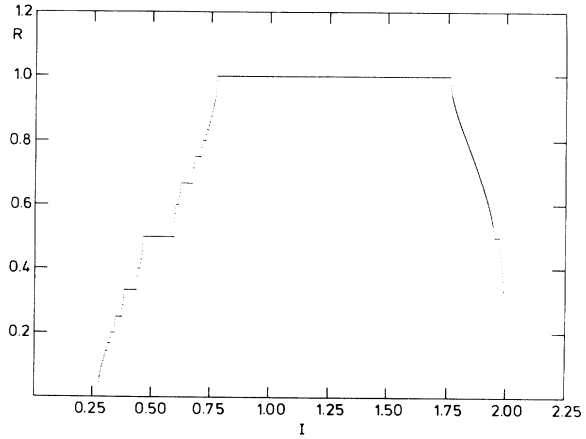

FIG. 6. The firing number R as function of I. The amplitude of the modulation is $A=0.1$. The other parameters are the same as in Fig. 5.

The attractor is stable when

$$|L|<1\ , \tag{18}$$

where the Lyapunov number can be written $L=\prod_{i=1}^{P}L_i^{1/P}$ as a consequence of the periodicity. The edges of a step are determined by a breakdown of one of these conditions. In the subcritical region of parameter space, the periodic attractor becomes unstable ($|L|=1$) on the edge of a step, while in other parts of the parameter space the edges may be due to some sort of catastrophe or crisis. In Fig. 2 some of the dominant steps, obtained numerically by Eqs. (17) and (18), are shown in (A,I) space. We notice that two steps with an identical firing number can exist if $R<R_{\max}$. For our particular choice of parameters the two 1/1 steps merge at a critical value of I, while steps with $R>1$ have not been observed in the subcritical region of parameter space.

For the $1/Q$ steps, Eq. (17) and the marginal stability condition $|L|=1$ can be solved analytically. The lower edge is given by

$$\left[\frac{A_0-A-I\tau_d}{B_0-I\tau_d}\right]^{\tau_d}\left[\frac{I\tau_u-B_0}{I\tau_u-A_0+A}\right]^{\tau_u}=\exp\left[\frac{2\pi}{\omega}Q\right]\ , \tag{19}$$

and the upper edge by

$$\left[\frac{I\tau_d-A_0-A}{B_0-I\tau_d}\right]^{\tau_d}\left[\frac{I\tau_u-B_0}{I\tau_u-A_0-A}\right]^{\tau_u}=\exp\left[\frac{2\pi}{\omega}Q\right]\ . \tag{20}$$

We note that in the limits $I\to(A_0-A)/\tau_u$ and $I\to B_0/\tau_u$ the denominator Q goes to infinity as expected.

The size of the steps increases in the subcritical region I, until the phase locking becomes complete on l_1 for $I<I_c$ and on l_2 for $I>I_c$. Figures 6 and 7 show the firing number and the Lyapunov exponents, respectively, as functions of I for $A=0.1$. For small values of I (region II) the phase locking is complete and $\lambda<0$ everywhere, while for bigger values of I (region I) both periodic ($\lambda<0$) and quasiperiodic attractors ($\lambda=0$) exist.

We emphasize that in the subcritical region I and on the critical lines the system is equivalent to a circle map of order 3, and hence has the same scaling properties [18]. In particular, the steps open with size $\Delta I\sim A^P$ for small A, and develop a complete devil's staircase with fractal dimension $D=0.87$ along the critical lines.

As the phase locking is already complete on l_1, the size of the steps cannot continue to grow in the complete phase locked region II. A knee [12] appears for $A=A_g$ at the "upper" edge of the step, i.e., the edge closest to $I_{\max}$, and the size of the step starts to decrease. While both edges for $A<A_g$ are determined by loss of stability $|L|=1$, this is for $A>A_g$ only true for the lower edge, while the upper edge is given by a breakdown of Eq. (17). After the appearance of the knee, the step size continues to decrease until the step vanishes for $(A,I)=(A_0-B_0,B_0/\tau_u)$. Everywhere in region II the steps

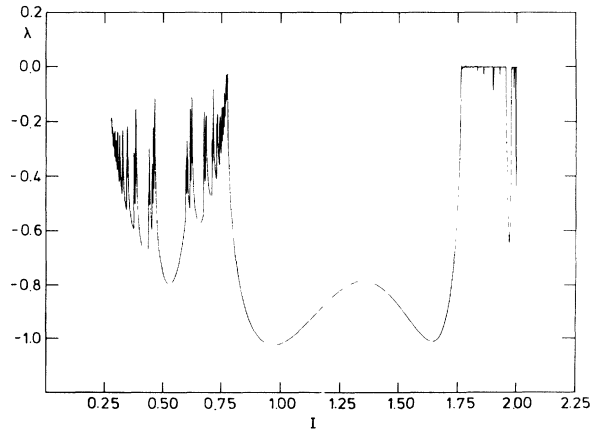

FIG. 7. The Lyapunov exponent λ as a function of I for the same parameters as in Fig. 6. In region II ($I<0.93$) all attractors are periodic, while in region I ($I>0.93$) both periodic and quasiperiodic attractors exist.

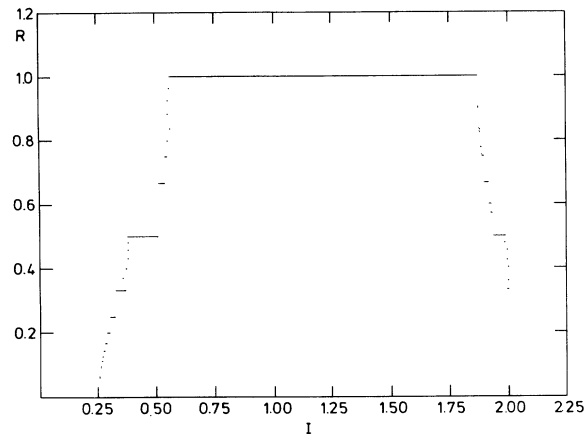

FIG. 8. The firing number R as a function of I. The amplitude of the modulation is $A=0.22$. The other parameters are again the same as in Fig. 5.

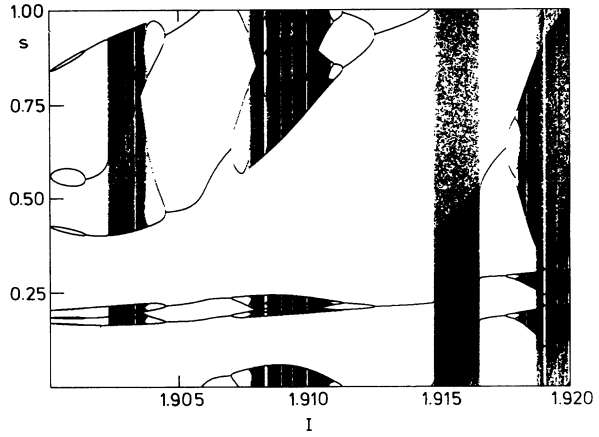

FIG. 10. The variable $s_i=t_i \mathrm{mod}(2\pi/\omega)$, $i=501, 502, \ldots, 1500$ as a function of I for the same parameters as in Fig. 8. The first 500 iterations have been discarded to avoid the transients. The usual scenario of periodic attractors borne by an inverse tangent bifurcation and destroyed by a cascade of period doublings is observed.

form a complete devil's staircase, but now with dimension $D=0$ [12].

For $I>I_c$ the steps start to overlap when l_2 is crossed and region III is entered. Figures 8 and 9 show the firing number and the Lyapunov exponent as functions of I for $A=0.22$. We note the positive Lyapunov exponent in region III ($1.68<I<2$). Figure 10 shows in this region $s_i=t_i \mathrm{mod}(2\pi/\omega)$ as function of I. Both chaotic attractors, created by period-doubling cascades, and periodic windows are seen.

Increasing the amplitude A even further, region IV is entered. Due to the existence of both a gap and a noninvertibility in the return map, this region has a very complex structure. Depending on the exact position in parameter space, the gap may shadow the noninvertibility, and the CPL of region II is recovered. Elsewhere in region IV the period-doubling cascade caused by the noninvertibility may be interrupted as a result of the presence of the gap. Also several forms of crisis and intermittency are observed in this region. We will discuss these phenomena in detail elsewhere.

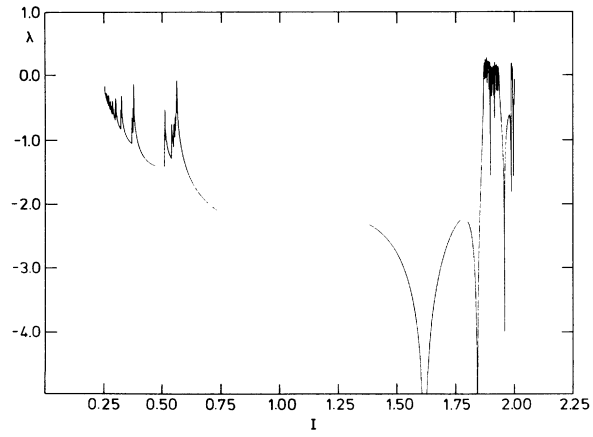

FIG. 9. The Lyapunov exponent λ as a function of I for the same parameters as in Fig. 8. In region II ($I<1.55$) all attractors are periodic, while in region III ($I>1.68$) both periodic and chaotic attractors exist.

We now consider the region $I<I_{\max}$ for the amplitude A close to the maximum A_0-B_0. In the limit $A\to A_0-B_0$ we must demand for $R<1$ the slope of the voltage to vanish just after a firing on the lower threshold, i.e., $V(t_i^+)=0$ or $I=B_0/\tau_u$. This is necessary in order for V to pass the narrow channel between the upper and the lower threshold at $t=\pi/2$. From Eq. (19) we find the slope $dI/dA=[\tau_u(\exp(2\pi Q/\omega\tau_u)-1)]^{-1}$ of the lower edge of the $1/Q$ step. The upper edge is given by a breakdown of Eq. (17) due to the collision of the voltage V and the lower part of the modulated upper threshold. From this criterion we find the slope $dI/dA=(\tau_u\{\exp[2\pi(Q-1)/\omega\tau_u]-1\})^{-1}$ of the upper edge of the $1/Q$ step ($Q\neq 1$). Hence, the size of the $1/Q$ steps disappears linearly in $dA=A-A_0+B_0$. All other steps with $R=P/Q<1$ are squeezed between the upper edge of the $1/Q_+$ step and the lower edge of the $1/Q_-$ step, where Q_+ is the lowest integer larger than Q/P and Q_- is the largest integer less than Q/P. The size of these steps will therefore vanish faster than linear in dA. Numerical work for $R>1$ shows that the same is true for steps with $Q>1$ and $P>Q$.

In the hatched region of Fig. 2 new harmonic steps are born. When A approaches A_0-B_0, higher harmonics are created successively and the firing number goes to infinity. Thus, for $I<I_{\max}$, the parameter space will be dominated by the harmonic steps for A close to A_0-B_0.

For the region $I>I_{\max}$, conclusions analogous to the above cannot be drawn due to the possibility of overlapping steps. However, numerically it is observed that for A close to A_0-B_0 the harmonic steps are strongly dominant in this region too.

VI. SUMMARY AND DISCUSSION

We have analytically and numerically explored the parameter space of a relaxation oscillator with a finite resetting time. Two critical lines divide the parameter space into four regions of qualitatively different behavior. In the subcritical region, i.e., for weak nonlinearity, the attractors are either periodic or quasiperiodic. Increasing the nonlinear parameter A, either a region of complete phase locking or a chaotic region is encountered, depending on the exact values of the parameters. While the return map is one-to-one in the subcritical region it is multivalued (with one branch hidden by the gap) or noninvertible in the supercritical regions. Increasing the amplitude further, the second critical line is crossed and the return map becomes both multivalued and noninvertible. In this region both complete phase locking and chaos exist.

In the weak nonlinear region $A \ll 1$, the dominant phase-locked regions are the $1/Q$ steps. As the nonlinearity grows, new steps are born and the maximum value of the rotation number R increases. The size of the steps with $R < 1$ decreases to vanish for $A = A_0 - B_0$, where the harmonic steps now dominate.

We close the paper with a comparison against related models. In Ref. [12] the same model was studied with zero resetting time ($\tau_d = 0$). The dominant contrast is the absence of a chaotic region. Only one critical line exists, leaving the phase locking complete for sufficiently strong nonlinearity. This difference is due to the fact that with the abrupt resetting the return map is an inverse circle map. It is the finite slope of the resetting voltage that creates a noninvertibility in the return map, and hence makes the chaotic attractors possible. We notice that if the resetting time is finite, a chaotic region III can always be found for A close to $A_0 - B_0$ and for I close to B_0/τ_d, although the area of this region vanishes as τ_d goes to zero. However, the existence of region IV requires $A_c < A_0 - B_0$, and consequently that τ_d exceed a positive threshold.

A model with the potential for both complete phase locking and chaos was considered in Ref. [13]. Here modulation was introduced on the upper and lower thresholds while the abrupt resetting was retained. Although both a region of complete phase locking and a chaotic region exist in parameter space, a region where these behaviors coexist is not found. The reason for this is revealed by considering the return map: the gap associated with the complete phase locking will cover the eventual noninvertibility and kill any attempt at chaotic behavior.

Thus the present model is an integrate-and-fire system that shows simultaneously a gap and a noninvertibility in the underlying return map. This complexity gives rise to some interesting forms of intermittent behavior and of sudden changes (crises) in the structure of the attractors. The details of these phenomena will be reported elsewhere.

ACKNOWLEDGMENTS

The authors are deeply grateful to Professor P. Alstrøm and Professor M. T. Levinsen, University of Copenhagen, for very helpful discussions and suggestions. Five of us (D.-R. H., S. H., M. B., U. K., and W. M.) were supported by Deutsche Forschungsgemeinschaft via the Sonderforschungsbereich 185 "Nichtlinear Dynamik." One of us (D.-R. H.) was also supported by M. E. Hereaus Stiftung.

*Permanent address: CCAST (World Laboratory), Beijing 100080, People's Republic of China. Mailing address: Department of Physics, Northwestern University, Xian 710069, People's Republic of China.

[1] P. Alstrøm and M. T. Levinsen, Phys. Rev. B **40**, 4609 (1989).
[2] J. Maselko and H. L. Swinney, J. Chem. Phys. **85**, 6430 (1986).
[3] R. J. Bagley, G. Mayer-Kress, and J. D. Farmer, Phys. Lett. **114A**, 419 (1986).
[4] J. F. Fohlmeister, Kybernetik **13**, 104 (1973); P. Alstrøm and M. T. Levinsen, Phys. Lett. A **138**, 127 (1988).
[5] L. Glass and M. C. Mackey, J. Math. Biol. **7**, 339 (1979).
[6] P. C. Bressloff and J. Stark, Phys. Lett. A **150**, 187 (1990).
[7] P. Martien, S. C. Pope, P. L. Scott, and R. S. Shaw, Phys. Lett. A **110**, 399 (1985).
[8] P. A. Bernhardt, Physica D **52**, 489 (1991).
[9] A. Cumming and P. S. Linsay, Phys. Rev. Lett. **59**, 1633 (1987).
[10] P. Alstrøm and M. T. Levinsen, Phys. Lett. A **128**, 187 (1988).
[11] P. Alstrøm, B. Christiansen, and M. T. Levinsen, Phys. Rev. Lett. **61**, 1679 (1988); Phys. Rev. A **40**, 7239 (1989).
[12] P. Alstrøm, B. Christiansen, and M. T. Levinsen, Phys. Rev. B **41**, 1308 (1990).
[13] B. Christiansen, P. Alstrøm, and M. T. Levinsen, Phys. Rev. A **42**, 1891 (1990).
[14] Da-Ren He, Da-kay Wang, Kang-Jie Shi, Cheng-hai Yang, Lai-yuan Chao, and Ji-Yue Zhang, Phys. Lett. A **136**, 363 (1989); Bull. Am. Phys. Soc. **33** (3), 243 (1988); **34** (3), 689 (1989); **35** (3), 353 (1990).
[15] Ji Feng, Liu Hui, Yang Zheng-hai, Kang-Jie Shi, Da-Ren he, and Da-Kai Wang, Chin. Phys. Lett. **1**, 1 (1991).
[16] See, e.g., R. Thom, *Structural Stability and Morphogenesis* (Benjamin, Reading, MA, 1975), Chap. 5.
[17] The exponent λ is the Lyapunov exponent per iteration of h. Multiplying by the firing number R gives Lyapunov exponent per time unit.
[18] S. J. Shenker, Physica D **5**, 405 (1982); M. J. Feigenbaum, L. P. Kadanoff, and S. J. Shenker, *ibid.* **5** 370 (1982); D. Rand, S. Ostlund, J. Sethna, and E. Siggia, Phys. Rev. Lett. **49**, 132 (1982); Physica D **8**, 303 (1983).

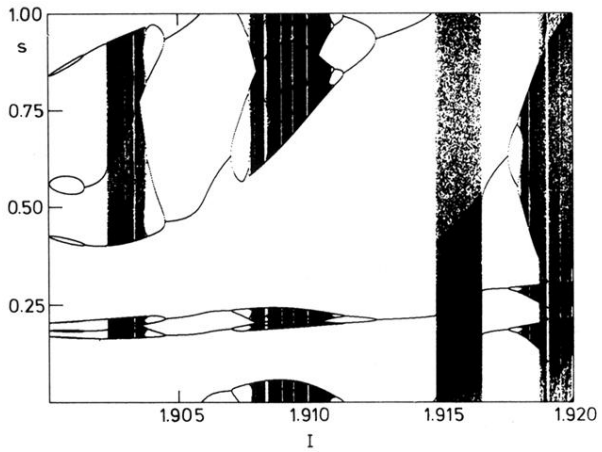

FIG. 10. The variable $s_i = t_i \bmod(2\pi/\omega)$, $i = 501, 502, \ldots, 1500$ as a function of I for the same parameters as in Fig. 8. The first 500 iterations have been discarded to avoid the transients. The usual scenario of periodic attractors borne by an inverse tangent bifurcation and destroyed by a cascade of period doublings is observed.